Single-lap joint creep behaviour of two soft adhesives

Estève Ernault, Julie Diani, Quentin Schmid

Preprint

Single-lap joint creep behaviour of two soft adhesives

Estève Ernault[1], Julie DIANI[1*], Quentin Schmid[2]
[1]*Laboratoire de Mécanique des Solides, École Polytechnique, Palaiseau, France*
[2]*Centre de Recherche Rhône-Alpes (CRRA), Pierre-Bénite, France*
[*]Corresponding author: julie.diani@polytechnique.edu

Single-lap joint creep behaviour of two soft adhesives

Abstract: Two hot melt pressure sensitive adhesives have been submitted to bonded joint creep tests. An amorphous and a semicrystalline adhesives have been considered for their different microstructures leading to different mechanical behaviors. The adhesives are referred as soft since their glass transition temperatures stand well below the temperatures of applications, resulting in low stiffnesses. The creep of structural joints has been characterized with single-lap joint tests. Two types of adherends were considered either glass or stainless steel. The adherend roughness and the adhesive wettability have been characterized before testing. The significant stiffness contrast between the stiff adherends and the soft adhesives promoted homogeneous simple shear creeps. The amorphous adhesive showed creep behaviors that depend on the type of substrates, showing that the joint viscoelasticity could not be predicted knowing the bulk adhesive viscoelasticity only, unlike for stiff adhesives as recently reported in the literature. Finally, the SLJ creep behaviors of both adhesives on the same glass adherends were compared and discussed at the light of their different microstructures inducing different mechanical behaviors.

Keywords: soft adhesives; single-lap joint; creep; viscoelasticity

1.Introduction

Hot melt pressure sensitive adhesives (HMPSA) are a class of bonding materials commonly used in the industry to prevent sewing, riveting, bolting... of two substrates. The range of applications is extremely wide, from diapers to the aeronautic industry. In this competitive segment, an ideal HMPSA allies low cost, aging stability, ease of process and targeted performance of adhesion, the latter being often assessed by the single-lap joint (SLJ) test. While single-lap joints create analysis difficulties when the test temperature is below the adhesive glass transition temperature[1-3], they become convenient structures for simple shear tests when the adhesive is soft due to testing temperatures above its glass transition temperature. Characterizing the creep behavior of structural adhesive joints is common.[4-6] Other studies have also characterized the time-dependent behavior of bulk adhesives[7,8] However, very few studies tried to bridge the gap between the viscoelasticity of the bulk adhesive and the viscoelasticity of the adhesive joint. In the case of a stiff adhesive, below its glass transition temperature, Saeimi Sadigh et al.[9,10] reproduced single-lap joint creep tests successfully knowing the viscoelastic behavior of the bulk adhesive when considering one type of adherend. The objective of the current contribution is to possibly extend such a result considering two soft HMPSA and two types of adherends. Actually, few studies have considered soft adhesives, that differ from stiff adhesives for their very low long-term elastic modulus and strong time-dependent behavior. Even fewer studies have looked at the creep behavior of soft adhesives, and when it was done the focus was set on the impact of the environment and of possible aging.[11-13]

Two adhesives differing in their chemical and physical structures are considered. One material is an amorphous styrene-butadiene-styrene based polymer used for disposable hygienic products, such as diapers, while the second one is a semicrystalline polyolefin entering in the manufacturing of cushioned envelopes. The bulk adhesives were first characterized running differential scanning

calorimetry measures, dynamic mechanical analysis tests and simple uniaxial tension tests. As mentioned earlier, Saeimi Sadigh et al.[9,10] were able to predict the single-lap joint creep of a stiff adhesive simply knowing the bulk adhesive viscoelasticity, and therefore without accounting for the adherend type. This result will be explored here by characterizing the SLJ creep of the amorphous adhesive layered between either glass or stainless steel adherends. The comparison between the SLJ creep behaviors will allow discussing the impact of the type of adherend on the adhesive creep response. Finally, the SLJ creep behaviors of the viscoplastic semicrystalline adhesive and of the viscoelastic amorphous one are compared in order to study the impact of the bulk material mechanical behavior on the adhesive response.

2. Materials

2.1. Adhesives

Two commercial hot melt pressure sensitive adhesives were provided by Bostik. Material A1 is an amorphous styrene-butadiene-styrene based polymer, and material SC1 is a semicrystalline polyolefin. Both materials were chosen for their different chemical and physical microstructures while still being processed and applied at similar temperatures when used. Note that the exact chemical compositions of A1 and SC1 cannot be disclosed. However, enough information will be provided to analyze the mechanical responses of the adhesives. These adhesives were delivered as adhesive films and as bulk dog-bone samples.

The HMPSA thermal transitions have been characterized by modulated temperature differential scanning calorimetry (MT-DSC). Samples of 5 to 10 mg have been encapsulated in aluminum crucibles and submitted to an isotherm of 2 hours at 144 °C in order to repeat the thermal history applied to single-lap joints. Two heating ramps were performed at 2 K/min from -78 °C to 157 °C with modulated amplitudes of ± 0.5 K over periods of 60 s with the Netzsch Polyma 214 DSC. Two empty crucibles were submitted to the same experimental procedure in order to generate a reference baseline. It has been noticed that signals from the first and second heating ramps were similar, indicating the reversibility of the changes of states occurring in the applied temperature range, and the fact that no residual stresses were left after the 2 hours exposure at 144 °C. Therefore, only the MT-DSC reversing and non-reversing signals of the second heating ramp have been displayed in Figure 1.

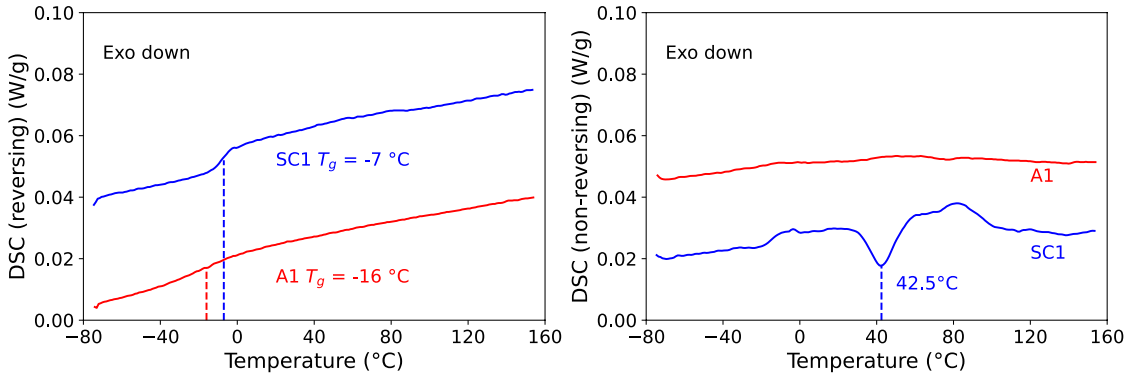

Figure 1. MT-DSC reversing and non-reversing signals obtained during the second heating ramps at 2 K/min with modulation amplitude of ± 0.5 °C over 60 s periods.

The material glass transition temperatures stand below the room temperature as shown by the reversing signals in Figure 1. Note that albeit co-polymers may exhibit two glass transition temperatures, HMPSAs show regularly one glass transition temperature only, due to their formulations rich in tackifying resin, plasticizers and other additives. [14, 15, 16] The non-reversing MT-DSC signal displays kinetic reactions such as melting or crystallization. Polyolefin based SC1 shows melting-crystallization phase transition with a melting peak above 40 °C, whereas nothing is visible for the amorphous styrene-butadiene-styrene based A1.

The single-lap joint tests were chosen to be performed at 40 °C (±1 °C) in order to deal with soft rubbery-like adhesives. In order to assess the rubbery states of the adhesives at such a temperature, the bulk adhesives were submitted to dynamic mechanical analysis (DMA) temperature sweeps. Slender rectangular samples were submitted to sinusoidal torsion tests at 0.1% strain amplitude and 1 Hz during a temperature ramp of 2 °C/min. The tests were run on an Anton Paar MCR 502 rheometer. Figure 2 presents the shear storage modulus and damping factor (loss over storage moduli) for each material. The storage moduli drop from values above 1 000 MPa in the glassy state at low temperatures to values of the order of the MPa in the rubbery state at higher temperatures. It appears that at 40 °C, both materials are close to the rubbery state, displaying low storage modulus values of a few MPa for the semicrystalline adhesive and of less than 1 MPa for the amorphous one.

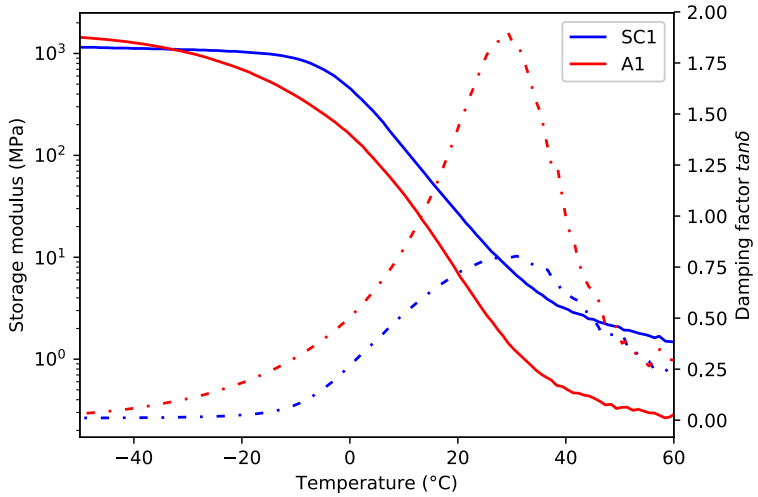

Figure 2. Storage modulus (solid line) and damping factor (dashed dotted line) recorded during temperature sweep torsion dynamic mechanical analysis test at 0.1% strain and 1Hz for a temperature ramp of 2 °C/min.

It is well known that the adherend roughness may impact the behavior of adhesive single-lap joints.[17, 18, 19] It has been also documented that HMPSA wettability has an impact on SLJ shear strength.[18, 19, 20] Therefore, in the next two sections, the adherend roughness and flatness have been gauged by profilometry, and the adhesive wettability has been assessed measuring the contact angle of a drop on the adherends.

2.2. Adherend roughness and flatness

The adherend surfaces have been characterized with a Veeco Dektat 150 profilometer with a diamond tip stylus of 2 µm applied with a 2 mg weight. Data were collected every µm in the X direction and every 20 µm in the Y direction. Figures 3 (resp. 4) shows the maps of the depths, and the profiles of the depth deviations from the average depth along the lines drawn on the maps for the glass (resp. stainless steel) plates. The adherend roughness was assessed by the arithmetical mean deviation of the roughness profile, noted $\overline{R_a}$ and calculated according to,

$$\overline{R_a^\alpha} = \frac{1}{l}\int_0^l |Z(\alpha)| d\alpha \quad \text{for } \alpha \in \{X, Y\} \tag{1}$$

Where l is the profile length, 12 mm in our case, and Z the depth deviation along X or Y profiles as displayed in Figures 3 and 4. Values of $\overline{R_a}$ calculated with Eq. (1) are listed in table 1. The stainless-steel plates appear slightly rougher than the glass plates. However, the difference is slim enough to be negligible.[18]

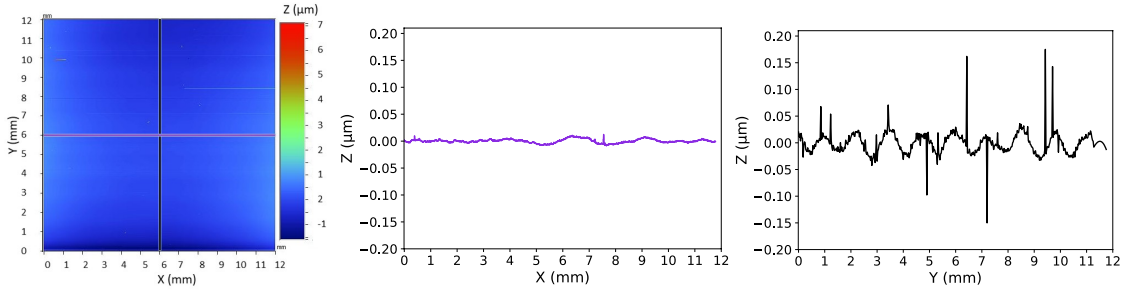

Figure 3. Profilometer glass plate depth mapping, and depth profiles along X and Y for the lines drawn on the map.

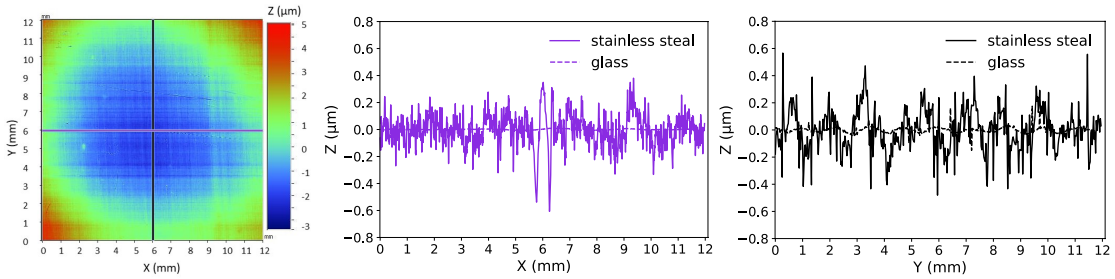

Figure 4. Profilometer stainless steel plate depth mapping, and depth profiles along X and Y for the lines drawn on the map.

The adherend flatness may affect also the strengths of single-lap joints since the adhesive thickness is known to have a significant impact.[21,22,23] Therefore, the adherend flatness has been quantified by the values of R_t defined by the distance between the highest peak and the lowest valley of the absolute depth measured along a given direction (Figure 5). Values are reported in Table 1. One notices that glass plates are flatter than the stainless-steel plates. However, the difference is lower than 3 µm, which should be negligible compared to the adhesive thicknesses of the order of 100 µm.

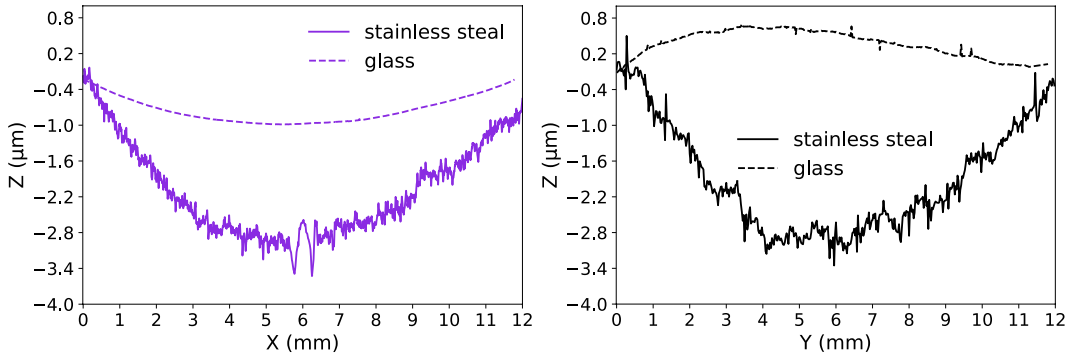

Figure 5. Comparison of the adherend absolute depths along the X and Y directions drawn on the profilometer maps Figures 3 and 4.

Table 1. Adherend average roughness $\overline{R_a}$ and flatness $\overline{R_t}$ in (μm) for maps and profiles displayed in Figures 3 to 5.

	Glass	Stainless steel
X profile roughness	0.003	0.090
Y profile roughness	0.015	0.120
X profile flatness	0.79	3.49
Y profile flatness	0.82	3.85
Maximum flatness value	2.13	4.18

2.3. Wettability

The wetting characteristics of A1 and SC1 HMPSA have been evaluated thanks to contact angle measurement using an optical tensiometer from Biolin Scientific. Since HMPSA cannot be placed as a liquid droplet, solid HMPSA balls of 2.5 ± 0.5 mg have been put on the glass or stainless-steel plates heated at 144 °C. The contact angles have been measured after the HMPSA ball formed a droplet (Figure 6) due simply to the high temperature. Note that the shape of the droplet remained rather constant over time. The mean contact angles and standard deviation were determined by averaging contact angles over five droplets (Table 2).

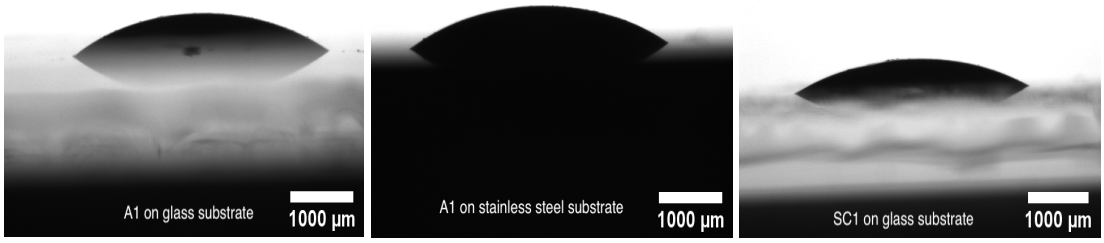

Figure 6. Contact angle images for droplet of HMPSA A1 on glass and stainless steel and HMPSA SC1 on glass, substrates being heated at 144 °C.

Table 2. Contact angles for A1 adhesive on glass and stainless steel substrates and for SC1 adhesive on glass substrates. Substrates have been heated at 144°C.

	Glass	Stainless steel
A1 average contact angle (°)	27.76 ± 0.28	37.55 ± 0.16
SC1 average contact angle (°)	23.36 ± 0.23	

For adhesive A1, the contact angle measured on glass plates is significantly lower, showing evidence of better wetting on the glass substrate. The ratio of surface energy of the glass substrate over the surface energy of the stainless-steel substrate appears to be in favor of the glass substrate reaching a value of approximately 1.1.[24] Last, the contact angle values of SC1 and A1 on glass are very similar, which will allow to discard the wettability as an impactful parameter when the behavior of both adhesives will be compared.

3. Single-lap joint creep experiments

3.1. Sample preparation

Glass and stainless steel adherends have been carefully cleaned with acetone. Adhesive bands of 25 mm width and 12.5 mm overlap length were set on the bottom adherend and covered by the top adherend in a single-lap joint manner. Note that a mold has been milled in order to help with the alignment of the top and bottom adherends. The joints were exposed to a temperature of 144 °C for 2 hours before applying a 2 kg roller. This procedure was chosen to match with some actual applications. The high temperature exposure enhances the adhesive wettability favoring cohesive fracture of the joints. Then, joints were let to cool down and tested the next day.

The joint adhesive thickness depended on the adhesive film thickness and on the pressure applied, which also explained the use of a roller. Before testing, the joint adhesive thicknesses have been measured with a Keyence microscope. The adhesive thickness was 145 ± 50 µm for joint A1 and 95 ± 10 µm for joints SC1 The adhesive thickness may impact the SLJ joint strength.[25] Therefore, it was verified that no correlation could be drawn between the adhesive thickness and the SLJ creep for the results that will be presented in the results section. Note that it was noticed that when the adhesive thickness went down to 60 µm, well out of the range of thicknesses considered here, the SLJ creep increased dramatically inducing early failures.

3.2. Creep test

The single-lap joint creep tests were run on an Instron 5967 tensile machine equipped with a thermal chamber regulated at 39 °C. For material A1, a constant weight of 1.5 kg corresponding to a shear stress of 0.046 MPa was suspended. One of the adherends has been held fixed while a constant weight $P = mg$ has been attached with a thread to the other adherend (Figure 7). The weight was sustained on a micrometer platform until applied almost instantaneously. The relative displacements of the adherends were recorded by image analysis. For this purpose, a speckle was drawn on the edges of the steel or glass adherends and numerical square markers were defined along the overlap length L as shown in Figure 7. The locations of the centers of the markers x_n were followed using the Vision module from Labview, and eight optical gauges were defined by $d_n = x_{2n} - x_{2n-1}, \forall n \in \{1,8\}$. Figure 8 displays, at a random given time, an example of the normalized gauge shear strains, defined as the adherend relative displacement d_n over the adhesive thickness T, normalized by the average shear strain. The shear strain appears similar along the overlap length L due to the stiffness contrast between the stiff adherends and the soft adhesives, assessing the simple shear state of loading.

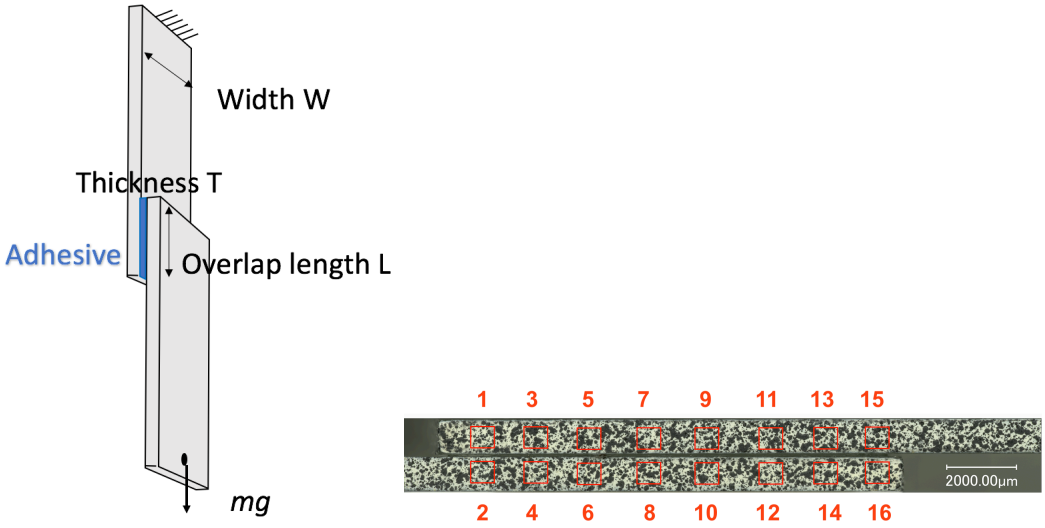

Figure 7. Scheme of the single-lap joint creep test and image of the joint rotated of 90 degrees, used to draw 16 optical markers defining 8 optical gauges following the adherend relative displacements along the joint overlap length.

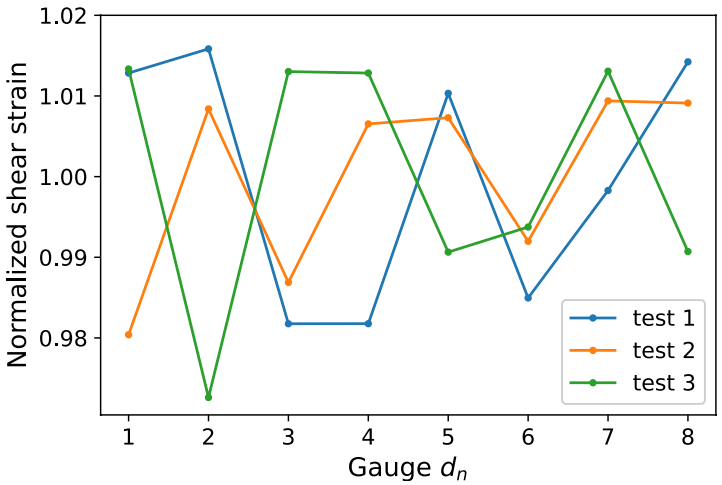

Figure 8. Example of shear strains recorded thanks to the optical gauges distributed along the single-lap joint overlap length L (Figure 7) and normalized by the average shear strain.

First, creep tests were run until failure in order to look at the post-mortem adherend surfaces and determine if the failure was cohesive, adhesive or mixed. Figure 9 illustrates an example of the shear strain at each gauge increasing with respect to time during creep. Since the curves superimpose, an average shear strain is defined,

$$\gamma(t) = \frac{1}{8}\sum_{n=1}^{8}\frac{d_n(t)}{T} = \frac{\langle d_n(t)\rangle}{T} \tag{2}$$

to characterize the shear strain submitted to the adhesive. Like in Djeumen et al.[6], three viscoelastic stages are recognized in Figure 9, that can be characterized by the strain rate. At the beginning of the creep test (after the load has been quasi-instantaneously applied), the shear strain rate decreases, then it remains constant and finally it increases dramatically.

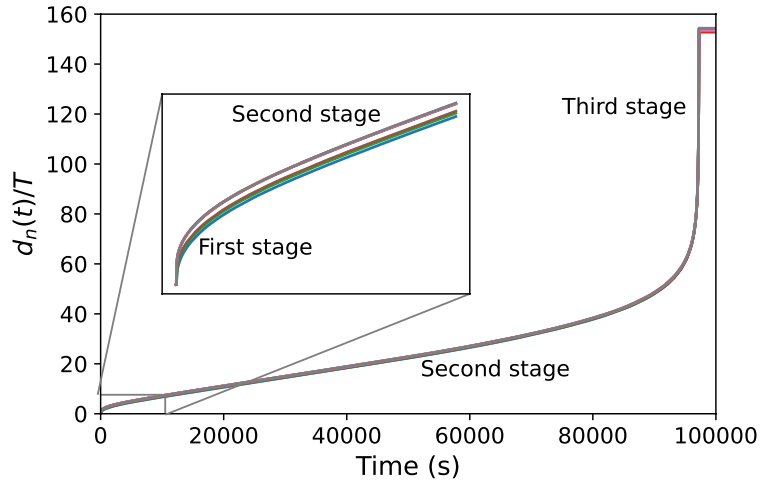

Figure 9. Increase of shear strain with respect to time of A1 adhesive on glass substrate submitted to a creep stress of 0.046 MPa.

The applied shear stress τ is defined as the weight over the adhesive initial area perpendicular to its thickness,

$$\tau = \frac{mg}{WL} \tag{3}$$

With W and L the adhesive width and overlap length (Figure 7). While the adhesive width W remains constant, the overlap length decreases with time as the adhesive debonds, resulting in an increase of the stress, and creep conditions are no longer valid. In the current study, our main interest was focused on creep behavior and therefore demanded to apply a constant stress. Therefore, the tests were limited to four hours in order to ensure that the applied stress was constant. Figure 10 shows a comparison the creep strain $\gamma(t)$ (Eq. (2)) over the applied stress τ (Eq. (3)) when the stress is evaluated as the engineering stress $\tau = \frac{mg}{W_0 L_0}$ and as the Cauchy stress $\tau = \frac{mg}{W_0 L(t)}$, W_0 and L_0 being the initial width and overlap length of the joint, and $L(t)$ the current overlap length. As one reads in Figure 10, the curves are close enough to validate the assumption of creep conditions.

Note that due to adhesive SC1 high stiffness, a 15 kg weight has been applied to the SC1/glass SLJ. The constant stress was maintained with the Instron 5967 tensile machine since the relatively thin glass plates could not hold such a weight attached to a thread without breaking. This technical change did not degrade the creep test accuracy.

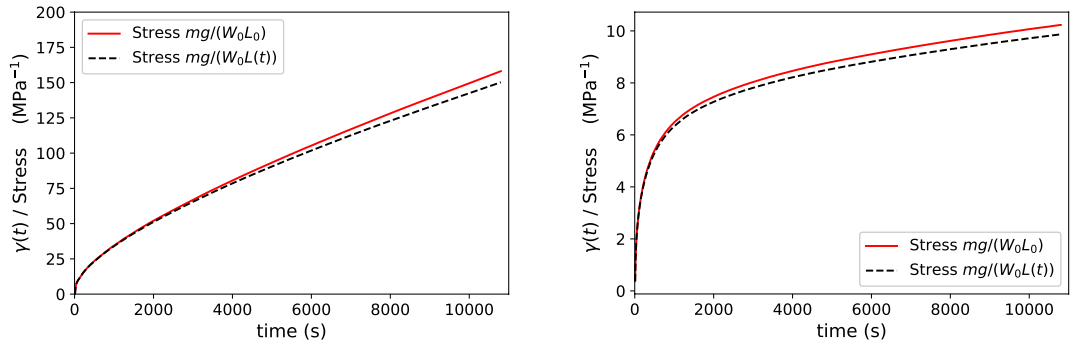

Figure 10. Comparison of A1 (Left) and SC1 (Right) SLJ creep responses plotted as the shear strain over the applied stress with respect to time when the applied stress is evaluated as the engineering stress or the Cauchy stress.

3.3. Impact of the joint geometry

Note that during the experimental campaign, it was noticed that creep results may be significantly scattered. This could be explained by the uncertainty of the soft joint dimensions. First, the adhesive thickness is not perfectly constant due to the product thickness as received and to the lap joint making process. Second, while the joint width and overlap length are rather accurately measured using an optic microscope for glass adherends, they are roughly evaluated for the steel adherends. Moreover, some cavities may appear while making the samples. Figure 11 shows an experimental result of normalized shear strain with respect to time during a creep test and the potential difference when errors are made of ±10% on the joint thickness and on both its thickness and area. Figure 11 shows that the geometrical uncertainties may generate quite some differences in the creep behavior. In order to circumvent this difficulty, it was noticed that the joint dimension uncertainties may be regrouped in an unknown parameter x when writing,

$$\frac{\gamma(t)}{\tau} = x \frac{WL}{T} \frac{\langle d_n(t) \rangle}{mg} \tag{4}$$

When needed, the parameter x (Eq. (4)) has been estimated in order to reach satisfactory reproducibility of the joint creep behavior.

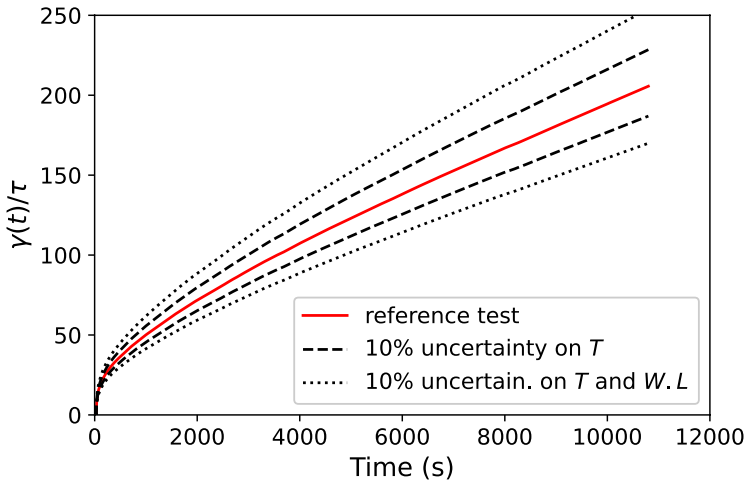

Figure 11. Illustration of the impact of joint thickness and area uncertainties on the creep behavior.

4. Results and discussion

4.1. Impact of the type of adherend on the SLJ creep

In order to test the impact of the type of adherend, creep tests were run on SLJ made with the A1 adhesive layered on glass and stainless-steel substrates. Figure 12 shows the shear strain with respect to time for both type of joints. It appears that the adhesive holds better on the glass substrate. The post-mortem analyses (Figure 13) show that some adhesive remains on both adherend surfaces, revealing cohesive failures for glass and steel substrates. One might recognize some lines along the direction of the mobile substrate displacement. Actually, the process of fracture has been observed when glass substrate was used. Cavities appear in front of the line, then coalesce in a similar fashion as witnessed by Sosson et al.[26]

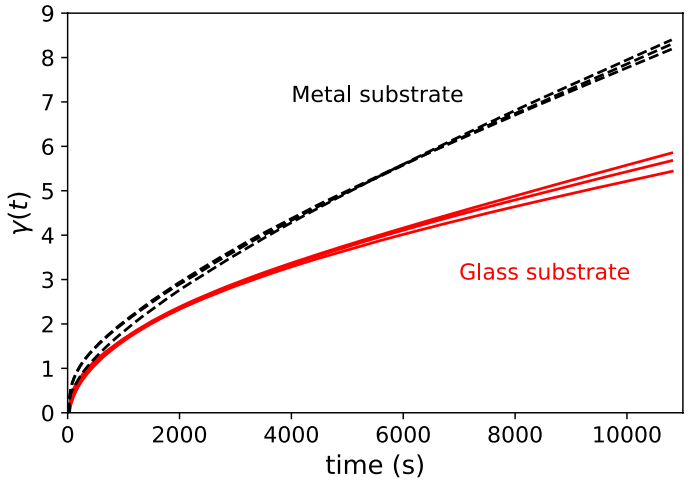

Figure 12. Shear strains with respect to time recorded during a SLJ creep tests of A1 adhesive on either glass or steel substrates

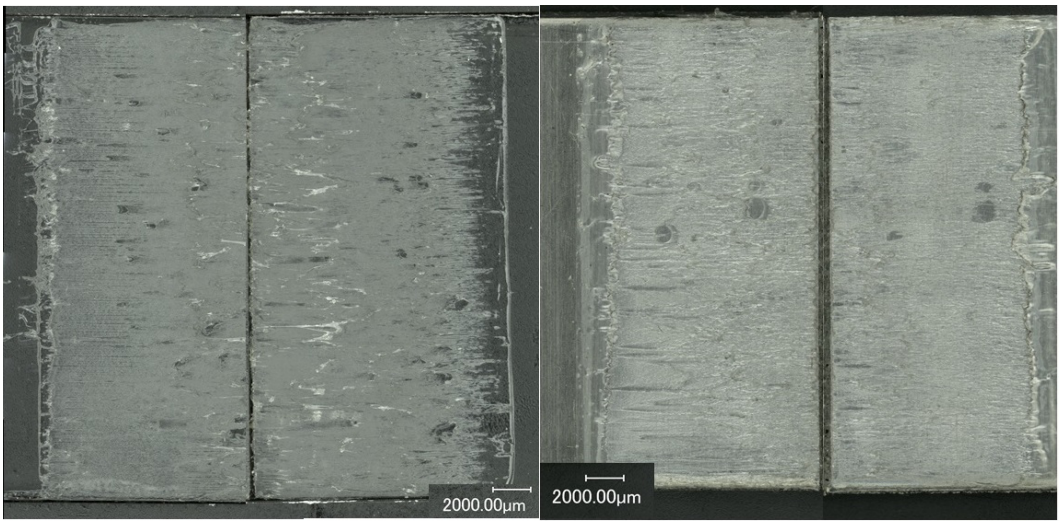

Figure 13. Post-mortem A1 single-lap joint adherends revealing cohesive failures for both glass and stainless steel adherends.

During the first four hours of the creep test, the shear strain is below 9%, which means that the adherend relative displacement is about 1 mm maximum for a joint overlap length of 12.5 mm. Consequently, the behavior shown in Figure 12 is driven mostly by the viscoelasticity of the adhesive and of the adhesive interphase. The adhesive strain increase with time is slower in the case of the glass adherends. This experimental observation might be explained by a better bonding of the adhesive on the glass. Actually, a better bonding could drive to a stiffer interphase driving to lower strain during the creep test. While this assumption would have to be further explored, running for instance creep tests with various thicknesses of adhesive, the difference of the adhesive surface wetting, evaluated thanks to contact angles (Table 2), supports this idea. The lower contact angle measured on glass is in favor of a better wettability on glass. However, the difference of chemical compatibility should also impact the bonding between the substrate and the adhesive.

More interestingly, the viscoelastic creep responses are different and therefore cannot be imputed to the viscoelastic behavior of the adhesive only. The viscoelastic behavior of the single-lap joint is probably dependent on the adhesive/adherend interphase which is expected to be viscoelastic too and dependent on the chemical and physical bonding. As a consequence, contrary to Saeimi Sadigh et al. [9, 10], it is impossible to predict the creep behavior of our single-lap joints by simply characterizing the bulk adhesive viscoelasticity. The interphase impact should logically be lessened for hard adhesives, which could explain the former results obtained in the literature.[9, 10] In the next section, the creep behavior of A1/glass and SC1/glass single-lap joints are compared.

4.2. Comparison of the SLJ creep of two different soft adhesives

Conventional uniaxial tension tests at room temperature revealed significant differences in the mechanical behaviors of bulk adhesives A1 and SC1, material SC1 being significantly stiffer and shows necking at large strain.

Figure 14 shows a comparison of the creep responses of both adhesives. At the beginning of the test, the strain rate is significantly larger for the SC1 adhesives. However, it rapidly decreases and become smaller than the A1 SLJ strain rate. Looking at this result, one could expect the semicrystalline adhesive to hold longer, which is not the case. Actually, the third stage of the creep (as displayed in Figure 9) happens for strains of about 10% for adhesive SC1 while it occurs at significantly larger strain (up to 40%) for adhesive A1. This surprising result might be due to the viscoplastic behavior of the semicrystalline polymer, displaying necking during classic monotonic uniaxial tension tests, which happens to be dramatic for any creep loading. Moreover, the post-mortem analysis of the glass adherends revealed a mixed adhesive/cohesive failure (Figure 15) which may explain the earlier complete debonding of the SLJ. The bubbles displayed

in Figure 15, where the adhesive failure is localized, have been witnessed consistently with adhesive SC1 despite similar wettability as A1 (Section 3.3). Therefore, while the semicrystalline adhesive is capable to sustain larger weight due to its larger stiffness, its ability to hold creep loadings is reduced compared to the amorphous adhesive.

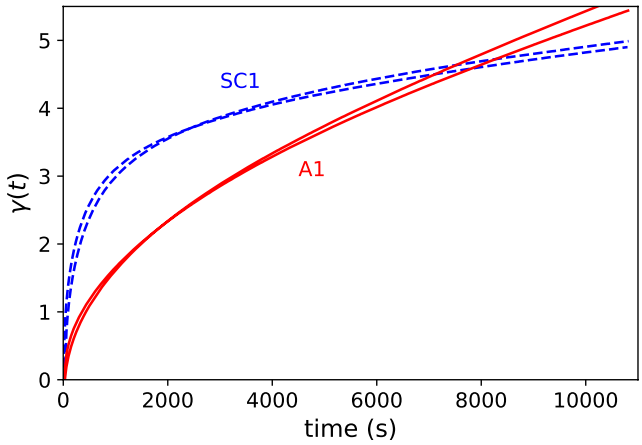

Figure 14. Comparison of the strain changes with respect to time for joints made of SC1 and A1 adhesives on glass substrates and submitted to creep tests.

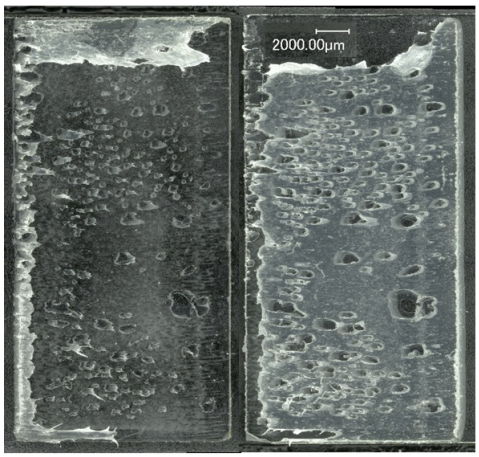

Figure 15. Mixed cohesive and adhesive failure of SC1 creep single-lap joint on glass adherends (scale bar of 2000 µm).

5. Conclusion

Results from the literature have shown that it was possible to predict the creep viscoelasticity of a hard glassy adhesive single-lap joint structure, by simply characterizing the viscoelasticity of the bulk adhesive. Actually, it could be expected that when the adhesive is in the glassy state, the adhesive interphase at the substrate/adhesive interface does not impact significantly the viscoleastic behavior of the joint. For soft adhesives, the interphase is more likely to impact the joint viscoelastic responses. In order to characterize such responses, two soft hot melt pressure sensitive adhesives single-lap joint structures have been submitted to creep tests. For this purpose, a constant weight was suspended while the shear strain was recorded with respect to time. First, using two different types of adherends, it has been shown that the viscoelastic creep responses of the amorphous adhesive is significantly impacted by the nature of the substrate. The glass and stainless-steel substrates have shown different wettability properties that might explain a better adhesion on the glass substrate, resulting in a better resistance to creep. In any case,

knowing only the viscoelasticity of the bulk adhesive is simply not enough to predict the soft joint creep response.
Second, when comparing the creep of a semicrystalline and an amorphous soft adhesives sandwiched between glass substrates, very different creep responses were obtained. The stiffer viscoplastic semicrystalline adhesive could hold larger weights. However, when comparing the shear strain with respect to time for similar shear strain, the semicrystalline adhesive shows better creep resistance at the beginning of the creep tests but early catastrophic failure that is probably due to its viscoplastic behavior exhibiting necking.
This study on creep behavior of soft HMPSA was able to show that characterizing the viscoelasticity of the bulk adhesive is not enough to predict its creep behavior within a simple single-lap joint structure. In the future, it could be interesting to use SLJ tests to estimate the viscoelasticity and the thickness of the substrate/adhesive interphase according to the polymer and the substrate natures.

Acknowledgements
The authors are in debt to the PIMM laboratory (Arts et Métiers ParisTech) for giving us access to their profilometer and to C. Gorny for helping us carrying out the roughness and flatness measures.
This action benefited from the support of the Chair Modeling advanced polymers for innovative material solutions led by the Ecole polytechnique (l'X) and the Fondation de l'Ecole Polytechnique and sponsored by Arkema.

References

[1] da Silva, L. F. M.; das Neves, P. J. C.; Adams, R. D.; Spelt, J. K. Analytical models of adhesively bonded joints\-Part I: Literature survey. *Int. J. Adhes. Adhes*. 2009, 29, 319–330.
[2] Cognard, J. Y.; Créac'hcadec, R.; Maurice, J. Numerical analysis of the stress distribution in single-lap shear tests under elastic assumption - Application to the optimisation of the mechanical behaviour. *Int. J. Adhes. Adhes*. 2011, 31, 715–724.
[3] Jouan, A.; Constantinescu, A. A critical comparison of shear tests for adhesive joints. *Int. J. Adhes. Adhes*. 2018, 84, 63–79.
[4] Allen, K. W.; Shanahan, M. E. R. The Creep behavior of structural Adhesive Joints II. *J. Adhes*. 1976, 8, 43–56.
[5] Su, N.; Mackie, R. Two-dimensional creep analysis of structural adhesive joints. *Int. J. Adhes. Adhes*. 1993, 13, 33–40.
[6] Djeumen, E.; Chataigner, S.; Créac'hcade, R.; Sourisseau, Q.; Quéméré, M.; Court, J.; Sayed, F. Creep investigations on adhesively bonded fasteners developed for offshore steel structures. *Marine Struct.* 2020, 69, 102660.
[7] Yu, X. X.; Corcombe, A. D.; Richardson, G. Material modelling for rate-dependent adhesives. *Int. J. Adhes. Adhes*. 2001, 21, 197–210.
[8] Majda, P.; Skrodzewics, J. A modified creep model of epoxy adhesive at ambient temperature. *Int. J. Adhes. Adhes*. 2009, 29, 396–404.
[9] Saeimi Sadigh, M. A.; Paygozar, B.; da Silva, L. F. M.; Vakili Tahami, F. Creep deformation simulation of adhesively bonded joints at different temperature levels using a modified power-law model. *Polym. Test.* 2019, 79, 106087.
[10] Saeimi Sadigh, M. A.; Paygozar, B.; da Silva, L. F. M.; Martínez-Pañeda, E. Creep behaviour and tensile response of adhesively bonded polyethylene joints: Single-Lap and Double-Strap. *Int. J. Adhes. Adhes*. 2020, 102, 102666.
[11] Piccirelli, N.; Auriac, Y.; Shanahan, M.E.R. Creep behavior at high temperature of epoxy-imide/steel joints – Influence of environment on creep rate. *J. Adhes*. 1998, 68, 281-300.

[12] Tan, W.; Na, J.X.; Zhou, Z-F. Effect of temperature and humidity on the creep and aging behavior of adhesive joints under static loads, *J. Adhes.* 2022, in press https://doi.org/10.1080/00218464.2022.2044319
[13] Tan, W.; Na, J.; Zhou. Z. Effect of service temperature on mechanical properties of adhesive joints after hygrothermal aging. *Polymers* 2021, 13, 3741.
[14] Yuan, B.; McGlinchey, C.; Pearce, E. M. Explanation of tackifier effect on the viscoelastic properties of polyolefin-based pressure sensitive adhesives. *J. Appl. Polym. Sci.* 2006, 99, 2408–2413.
[15] Galan, C.; Sierra, C. A.; Gomez Fatou, J. M.; Delgado, J. A. A hot-melt pressure-sensitive adhesive based on styrene-butadiene-styrene rubber. The effect of adhesive composition on the properties. *J. Appl. Polym. Sci.* 1996, 62, 1263–1275.
[16] Akiyama, S. Phase behavior and pressure sensitive adhesive properties in blends of poly(styrene-b-isoprene-b-styrene) with tackifier resin. *Polymer*. 2000, 41, 4021–4027.
[17] Pereira, A. M.; Ferreira, J. M.; Antunes, F. V.; Bártolo, P. J. Analysis of manufacturing parameters on the shear strength of aluminum adhesive single-lap joints. *J. Mater. Process. Techn.* 2010, 210, 610–617.
[18] Boutar, Y.; Naïmi, S.; Mezlini, S.; Ben Sik Ali, M. Effect of surface treatment on the shear strength of aluminum adhesive single-lap joints for automotive applications. *Int. J. Adhes. Adhes*. 2016, 67, 38–43.
[19] Ghumatkar, A.; Budhe, S.; Sekhar, R.; Banea, M.; de Barros, S. Influence of Adherend Surface Roughness on the Adhesive Bond Strength. *Lat. Amer. J. Solids Struct.* 2016, 13, 2356–2370.
[20] Borsellino, C.; Di Bella, G.; Ruisi, V. Adhesive joining of aluminum AA6082: The effects of resin and surface treatment. *Int. J. Adhes. Adhes*., 2009, 29, 36–44.
[21] Banea, M. D.; da Silva, L. F. M., Campilho, R. D. S. G. The Effect of Adhesive Thickness on the Mechanical Behavior of a Structural Polyurethane Adhesive. *J. Adhes.* 2015, 91, 331–346.
[22] Li, G.; Lee-Sullivan, P.; Thring, R. W. Nonlinear finite element analysis of stress and strain distributions across the adhesive thickness in composite single-lap joints. *Compos. Struct.* 1999, 46, 395–403.
[23] da Silva, L. F. M.; Rodrigues, T. N. S. S.; Figueiredo, M. A. V.; de Moura, M. F. S. F.; Chousal, J. A. G. Effect of Adhesive Type and Thickness on the Lap Shear Strength. *J. Adhes*. 2006, 82, 1091–1115.
[24] Fowkes, F.M. Attractive forces at interfaces. *Ind. Eng. Chem.* 1964, 56, 40-52.
[25] da Silva, L. F. M.; Carbas, R. J. C.; Critchlow, G. W.; Figueiredo, M. A. V.; Brown, K. Effect of material, geometry, surface treatment and environment on the shear strength of single lap joints. *Int. J. Adhes. Adhes*. 2009, 29, 621–632.
[26] Sosson, F.; Chateauminois, A.; Creton, C. Investigation of shear failure mechanisms of pressure-sensitive adhesives. *J. Polym. Sci. Part B: Polym. Phys.*, 2005, 43, 3316–3330.